

Transverse beam size measurement system using visible synchrotron radiation at HLS II^{*}

TANG Kai()^{1;1)} SUN Bao-Gen()^{1;2)} YANG Yong-Liang()¹ LU Ping()¹
 TANG Lei-Lei()¹ WU Fang-Fang()¹ CHENG Chao-Cai()¹
 ZHENG Jia-Jun()¹ LI Hao()¹

¹ National Synchrotron Radiation Laboratory, University of Science and Technology of China, Hefei 230029, China

Abstract: An interferometer system and an imaging system using visible synchrotron radiation (SR) have been installed in HLS II storage ring. Simulations of these two systems are given using Synchrotron Radiation Workshop(SRW) code. With these two systems, the beam energy spread and the beam emittance can be measured. A detailed description of these two systems and the measurement method is given in this paper. The measurement results of beam size, emittance and energy spread are given at the end.

Key words: HLS II, interferometer, beam profile, beam energy spread, beam emittance

PACS: 29.20.db, 29.85.Ca, 29.90.+r

1 Introduction

Visible synchrotron radiation (SR) has been widely used for electron beam diagnostics in the storage rings. Overview of transverse beam profile diagnostic based emitted SR are given by Kube [1] and Takano [2] respectively. Beam diagnostic methods based SR can be classified in imaging methods, exploitation of SR wave-optics feature methods (such as π -polarization), projection methods and interference methods [3]. The measurement resolution is limited in a simple imaging system (using visual SR) due to diffraction effects [1]. However, a simple imaging system was still applied at the B8 beamline of HLS II [4] because the imaging system can monitor the beam state directly. Besides, HLS II is a second generation SR source with several hundreds μm transverse beam size both horizontal and vertical. Error results by those effect can be no more than 5%.

The SR interferometer is first applied to measure the beam size by Mitsuhashi at the ATF damping ring [5–8]. Now it has become a universal tool and has been applied in numerous facilities [9–18]. It was successfully demonstrated to measure a beam size of $39.0\mu\text{m}(H) \times 14.7\mu\text{m}(V)$ with a resolution better than $1\mu\text{m}$ [7]. T. Naito and T. Mitsuhashi [19] apply an interferometer with Herschelian reflective to reduce the disperse effect of the objective lens. By this method, the interferometer can measure a $4.7\mu\text{m}$ beam size. P. Chevtsov utilizes an interferometer to measure the beam energy spread by

ignoring the intrinsic beam size [9]. At HLS II, an interferometer system has been installed at the B7 beamline and a simple imaging system at the B8 beamline [4, 20].

With knowledge of the machine optical parameters and relative energy spread, the emittance can be inferred from the measured beam size [1]. Usually, the beam energy is not a constant and depends on beam current. So emittance is not a direct value. In this paper, a non-destructive method to measure beam energy spread and emittance simultaneously using these two systems is presented.

The configuration of these two systems are described in Section 2.1. The measurement method of the beam energy spread and the horizontal beam emittance using these two systems is described in Section 2.2. The simulation results computed by SRW [21] is given in 2.3. The measured result is given in Section 3.

2 Experimental methods

2.1 Experimental setup

HLS II is a second generation electron storage ring with an electron energy of 800 MeV. It has a fourfold periodicity with total eight 45° sector magnets, a circumference of 66 m, a design transverse beam emittance of $36.4\text{ nm}\cdot\text{rad}$ and a design relative energy spread of 4.7×10^{-4} . Tab.1 lists the beam parameters and the theoretic beam sizes at the B7 and B8 source point.

* Supported by National Natural Science Foundation of China (11105141, 11175173) and the upgrade project of Hefei Light Source

1) E-mail: tangkkai@mail.ustc.edu.cn

2) E-mail: bgsun@mail.ustc.edu.cn

©2013 Chinese Physical Society and the Institute of High Energy Physics of the Chinese Academy of Sciences and the Institute of Modern Physics of the Chinese Academy of Sciences and IOP Publishing Ltd

Table 1. Optics parameters and beam size of the B7 and B8 source point.

Parameters	B7	B8
$\beta_x(\text{m})$	1.7668	0.9235
$\beta_y(\text{m})$	12.3485	7.6854
$\eta_x(\text{m})$	0.1059	0.2793
η'_x	-0.1990	-0.4754
Design transverse $\varepsilon(\text{nm.rad})$	36.4	
Design energy spread δ	4.7×10^{-4}	
$\sigma_x(\text{mm})$ with 5% coupling	252.4	221.9
$\sigma_y(\text{mm})$ with 5% coupling	146.3	115.4
$\sigma_x(\text{mm})$ with 10% coupling	246.9	218.6
$\sigma_y(\text{mm})$ with 10% coupling	202.1	159.5

Fig. 1 shows the schematic layouts of the interferometer system. The SR is reflected 90° downwards by an oxygen-free copper mirror(mirror1) in the vacuum chamber. After reflected by Mirror2 and mirror3, the SR is transmitted to an optics table. On the optical table, the SR light is divided by the splitter1. The SR of these two channels passes through a double slit, an achromatic lens with 1000 mm focal length, a lens2 with 100 mm focal length, a polarizer and a 500 nm bandpass filter respective. The image is observed by a Procilica GE680 camera which is placed at the image plane.

The distance between the B7 source point and the double slit are 10.8 m for the horizontal channel and 11.1 m for the vertical channel. The slit separation is 5 mm and the size of the aperture is 0.5 mm × 2 mm($H \times V$) for the horizontal channel and 2 mm × 0.5 mm($H \times V$) for the vertical channel. With adjusting the place of Lens2 and the camera, we can magnify the pattern image by 3~5 ratios. The bandpass filter with a central wavelength at 500 nm and 10 nm FWHM bandwidth.

Fig. 2 shows the schematic layouts of the imaging system. Mirror1 is a water-cooled oxygen-free copper. Mirror2 ~ Mirror5 are reflect mirror. The achromatic lens has a focal length of 1400 mm. After reflected by a periscope layout(composed by mirror4 and mirror5), the SR is transmitted to an optics table. The lens2 is used to adjust the magnification of the imaging system.

The focal length of all lenses were measured. Local bump experiment was performed to measure the magnification of those two systems. The double slit was removed at the experiment. Experiments of dispersion function measurement were achieved by changing RF. Betatron functions used are theoretical value.

The camera has a CCD of 480 pixels × 640 pixels with pixel size of 7.4 μm × 7.4 μm. Experiment was performed to make sure that output property of the CCD is linear. Experiment were also performed by analysing the image obtained by the camera at different exposure time.

The results show that the beam size measurement result doesn't depend on the exposure time of the camera.

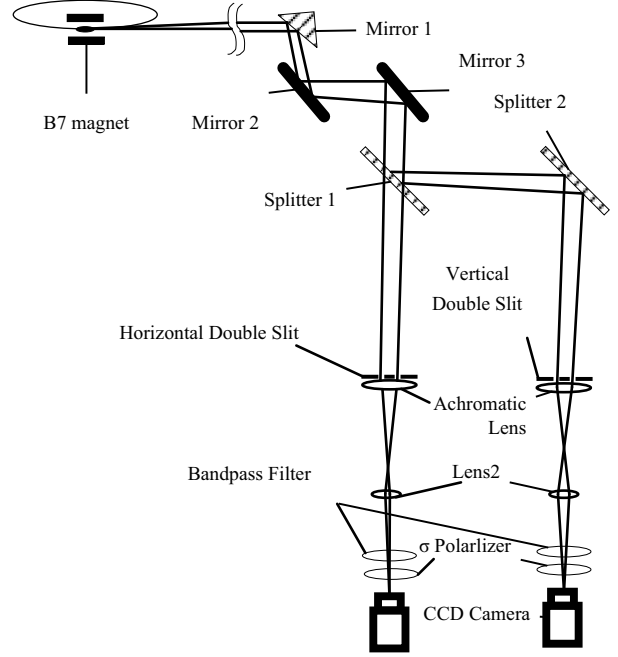


Fig. 1. Layout of the interferometer system at the B7 beamline

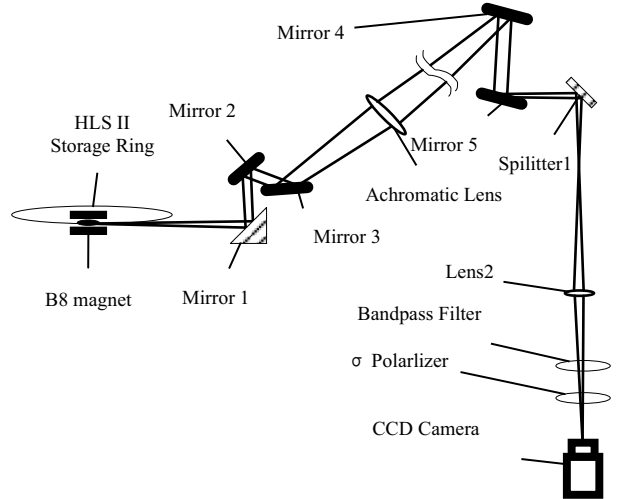


Fig. 2. Layout of the imaging system at the B8 beamline

2.2 Measurement theory

The theory of beam size measurement with interferometer is well-documented. It is a wavefront division two-beam interferometer using polarized quasi-monochromatic light. The SR wavefront is divided by a double slit and merge again at the image plane. Take the vertical channel as example, the fringe distribution [7] at the image plane is described by:

$$I(y) = I_0 \text{sinc}^2\left(\frac{\pi w_y}{\lambda L'} y\right) \left(1 + \gamma_y \cos\left(\frac{2\pi d_y}{\lambda L'} y + \phi_0\right)\right) \quad (1)$$

Where w_y denotes vertical size of the slit, L' denotes the distance between the double slits and the detector, d_y denotes the separation of the two slits, λ denotes the wavelength, ϕ_0 denotes the fringe phase, and γ_y denotes the complex degree of coherence. If the beam shape is a Gaussian profile [11], γ_y is given by:

$$\gamma_y = \exp\left\{-2\left(\frac{d_y\sigma_y}{\lambda L}\right)^2\right\} \quad (2)$$

Where σ_y denotes the beam size. Expanding Eq. (2):

$$\sigma_y = \frac{\lambda L}{\pi d_y} \sqrt{\frac{1}{2} \ln \frac{1}{\gamma_y}} \quad (3)$$

Reality, the fringe was fitted by function model below:

$$I(y) = a_1 \text{sinc}^2(a_2(y - a_5)) \{1 + a_3 \cos[a_4(y - a_6)]\} + a_7 \quad (4)$$

where sinc denotes $\sin(x)/x$ function, a_1, a_2, \dots, a_7 are fitting parameters. And a_3 is γ_y .

The theory of the transverse beam size measurement with the imaging system is simple. Ideally, the intensity profile monitored by camera would correspond to the beam profile at the source point scaled by the magnification factor of the system [15]. The vertical beam size is $115.4 \mu\text{m}$ and horizontal beam size is $221.9 \mu\text{m}$ (Table.1) when the coupling coefficient is 5%. Thus, the resolution limited by diffraction is far smaller than the beam size. With integrating the raw data along x direction and y direction respectively, two curves can be achieved. The beam size can be directly inferred by fitting these curves with function:

$$I(x) = a_1 \exp\left(-\frac{(x - a_2)^2}{2a_3^2}\right) + a_4 \quad (5)$$

where a_1 is related to light intensity, a_2 is the peak position of the curve and related to beam position, a_3 is the beam size, a_4 is related to the camera noise. The beam size is inferred by dividing a_3 by magnification ratio. This fitting model takes account of the camera noise and the background from stray illumination. An offset must be obtained if one fitted the profile with the Gaussian function.

Usually, the horizontal beam size has two sources: the portion due to betatron oscillation and the portion due to dispersion. Let ε_x denote horizontal beam emittance and δ denotes relative energy spread.

$$\varepsilon_x = \frac{\sigma_x^2 - \delta^2 \eta_x^2}{\beta_x} \quad (6)$$

Where β is betatron function and η is dispersion function. With subtracted the part due to dispersion, beam emittance can be inferred. Let $\sigma_\beta = \sqrt{\varepsilon_x \beta_x}$ denotes the size due to betatron oscillation and $\sigma_\delta = \delta \eta$ denotes the

size due to dispersion. For B8 source point, the $\sigma_\beta(178.9 \mu\text{m})$ can be compare to the $\sigma_\delta(131.3 \mu\text{m})$. For the B7 source point, the $\sigma_\delta(49.8 \mu\text{m})$ is far less than the $\sigma_\beta(247.4 \mu\text{m})$.

For the storage ring, the beam emittance and energy spread do not depend on the longitudinal position. Thus, horizontal beam emittance and energy spread at the B7 and B8 source point are the same. They can be described by:

$$\begin{cases} \sigma_{x,1}^2 = \varepsilon_x \beta_{x,1} + \delta^2 \eta_{x,1}^2 \\ \sigma_{x,2}^2 = \varepsilon_x \beta_{x,2} + \delta^2 \eta_{x,2}^2 \end{cases} \quad (7)$$

Where subscript 1 represent B7 and subscript 2 represent B8. We can solve for ε_x and δ from Eq. (7):

$$\begin{cases} \varepsilon_x = (\sigma_{x,1}^2 \eta_{x,2}^2 - \sigma_{x,2}^2 \eta_{x,1}^2) / (\beta_{x,1} \eta_{x,2}^2 - \beta_{x,2} \eta_{x,1}^2) \\ \delta = [(\sigma_{x,2}^2 \beta_{x,1} - \sigma_{x,1}^2 \beta_{x,2}) / (\beta_{x,1} \eta_{x,2}^2 - \beta_{x,2} \eta_{x,1}^2)]^{1/2} \end{cases} \quad (8)$$

After the horizontal beam sizes at the B7 and B8 source point measured simultaneously, the corresponding horizontal beam emittance and the beam energy spread can be inferred by Eq. (8).

2.3 Simulation Result

The SRW code can readily compute the SR emission [19]. The intensity distribution caused by a single electron is called filament-beam-spread function(FBSF). And the SR intensity distribution is computed by making a 2D convolution of the FBSF with a 2D Gaussian distribution profile.

The theoretical beam size at the B7 source point is $252.4 \mu\text{m}(H) \times 146.3 \mu\text{m}(V)$ (Tab. 1) and the corresponding degree of coherence are 0.3586 and 0.7007 respective when the coupling coefficient is 5%. The value of degree value of coherence(Tab. 2) can be inferred by fitting the simulated fringe with the function described in Eq. (4). The simulation γ_x is 0.6909 when the σ -polarized component of the SR is selected to illuminate the double slit and 0.6871 for π -polarized and 0.6825 for total SR. The simulation γ_y hardly depend on the polarity of SR.

Table 2. The degree of coherence simulated by SRW using different polarization component of the SR(theoretic value are 0.3586(H) and 0.7007(V)).

Parameters	σ -polarized	π -polarized	total
γ_x	0.3502	0.3503	0.3502
Relative error(%)	2.3	2.3	2.3
γ_y	0.6909	0.6871	0.6825
Relative error(%)	1.4	1.9	2.6

The simulated degree of coherence is less than the theoretic one(Tab. 1). Because the wavefront of SR was

sampled at a finite area so that some beam profile information is lost. Experiment of changing the sampling area size was performed. The bigger the sampled area is, the more accurate the simulation result will be.

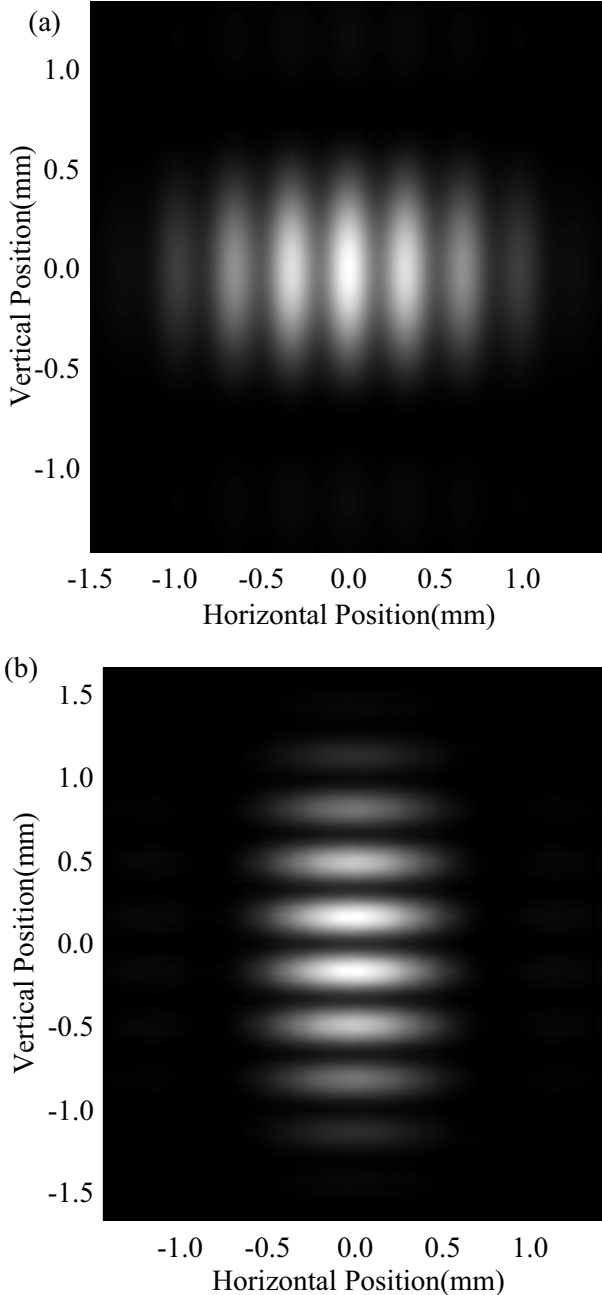


Fig. 3. The simulated(using SRW) intensity distribution of σ -polarization SR at the image plane of the interferometer system. (a)Horizontal channel assuming a finite beam ($\sigma_x = 253.4\mu m$). (b) Vertical channel assuming a finite beam ($\sigma_y = 149.9\mu m$)

For imaging system, the simulation FBSF is $17.4\mu m(H) \times 26.8\mu m(V)$. The simulation beam

size is $225.8\mu m(H) \times 122.2\mu m(V)$ for σ -polarization, $225.7\mu m(H) \times 127.8\mu m(V)$ for π -polarization and $225.7\mu m(H) \times 122.7\mu m(V)$ for total polarization. The simulation error for vertical direction of the imaging system has two sources: finite size of sampling area and fitting model error. The intensity distribution of imaging with π -polarized is a curve which has two peaks instead of Gaussian distribution. By comparing the simulation result with the theoretical value ($221.7\mu m(H) \times 118.3\mu m(V)$), we can reach the conclusion below:

- 1). The simulation result is in accordance with the theoretical value.
- 2). The simulation horizontal beam size hardly varies according to the polarity of SR.
- 3). The σ -polarization of SR should be utilized to measure the vertical beam size.

Thus, we select the σ -polarization of SR to measure the transverse beam size both for interferometer system and imaging system, both for horizontal size and vertical size.

3 Results and analysis

3.1 Measurement of beam size

In the usual operation of HLS II, coupling correction is performed with 4 skew quadrupoles in order to obtain a beam lifetime of 10 hour at 300 mA. The coupling coefficient is about 10%. Fig.4 and Fig.5 show fringes obtained by the vertical channel and the horizontal channel with a beam current of 100.4mA.

The raw data is a 2D matrix with 640 rows and 480 columns. And the data analysis is merely performed inside of a region of interest(ROI) area. Take vertical beam size analysis for instance. Set 11 columns data of the matrix which nearest to the peak position as the ROI area. With integrating the ROI along x direction, a vector which is similar with the blue curve as showed in Fig.4 can be obtained. By fitting the curve with Eq. (1) and taking into account that imbalance between the intensities on the double slit, γ can be inferred. The measured vertical beam size is $216\mu m(V)$ (Fig.4) and the horizontal beam size is $279\mu m$ (Fig.5).

The vertical beam size agrees with the theoretic value($212.0\mu m$) at 10% coupling coefficient. And the horizontal beam size is slightly larger than the theoretic value($246.9\mu m$). The reason might be the real energy spread is larger than the design value.

The possible error sources of the beam size measurement by the interferometer system contain the following aspect. Imperfection of the optic component and the finite pixel size of the CCD. Besides, the error of the distance between two slits(less than $1\mu m$), the slit size(less than $1\mu m$), the distance between the source portion and the double slit(10 mm), the nonlinearity of the CCD output(1.9% uncertainty) and the non-monochromatic

light(2% uncertainty) will also result in measurement error. At last, beam jitter can generate a phase shift in the fringe and will reduce the visibility of the fringe[14]. Assuming the beam offset from the orbit is $50\ \mu\text{m}$, we can get a visibility error of 1.7% and a horizontal beam size error of 1.4%. The horizontal beam size measurement error due to above cause is 3.0%.

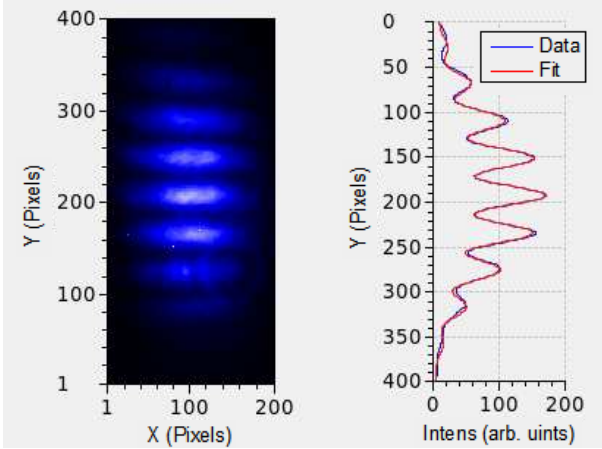


Fig. 4. A typical interference fringe obtained by the vertical interferometer using σ -polarized SR.

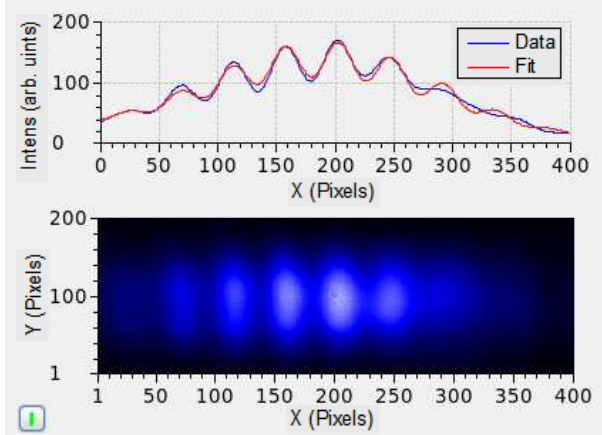


Fig. 5. A typical interference fringe obtained by the horizontal interferometer using σ -polarized SR.

Beam sizes of B8 source point were measured at single bunch operation. A set of background images was acquired at different beam current range. Exposure time should change in case of saturation or underexposure. A typical beam size measurement is $303\ \mu\text{m}(H) \times 174\ \mu\text{m}(V)$ (Fig.6) with a beam current of 4.3 mA. Measurement of beam size at different beam current was obtained(Fig.7). 100 images were acquired at each beam current. Measurement were repeated 3 times.

The vertical beam size(about $174\ \mu\text{m}$) agrees with the theoretic value($159.5\ \mu\text{m}$) and does not depend on the

beam current. But the horizontal beam size is far larger than the theoretic value and depends on the beam current. It was found in the measurement that the beam became unstable when the beam current was more than 8 mA.

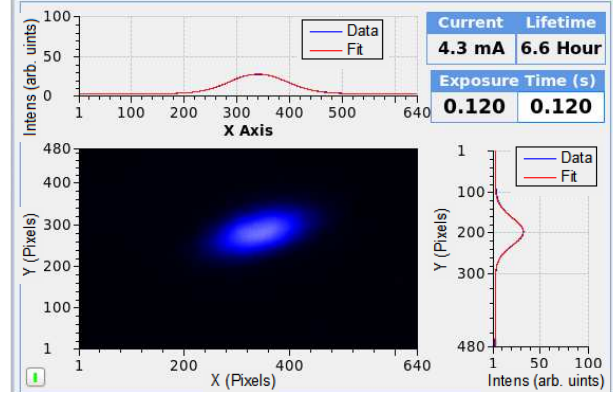


Fig. 6. The measured intensity distribution of σ -polarized SR at the image plane and the best fit. The beam current is 4.3 mA(at single bunch operation).

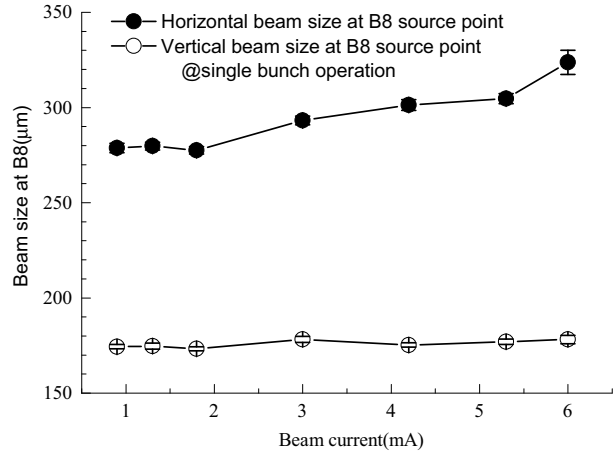


Fig. 7. The horizontal beam size and vertical beam size (± 1 standard deviation) measured by the imaging system.

3.2 Measuring beam energy spread and beam emittance

Horizontal beam sizes of the B7 and B8 source point were measured simultaneously at different beam current(from 80 mA to 240 mA with a step of 20 mA) at multi bunch operation(Fig. 8). The beam will be in the presence of longitudinal instability if the beam current is less than 80 mA. And the degree of coherence will be less than 0.2 if the beam current is larger than 240 mA.

The measured horizontal beam size of the B7 and B8 source point are far larger than the theoretic one. From Section 3.2, the measured energy spread is larger than

the theoretic value(4.7×10^{-4}). Besides, the horizontal beam size would be widened in the presence of a beam instability. From the performance of the feedback system of HLS II, we know that the transverse beam instability is reduced perfectly while the longitudinal beam instability is not reduced completely.

Statistics of the horizontal beam size of B8 source point(at 120 mA) show that the standard deviation is $7.5 \mu\text{m}$ and the range(maximum - minimum) is $35 \mu\text{m}$. Similarly, statistics of B7 show that the standard deviation is $1.5 \mu\text{m}$ and the range is $4 \mu\text{m}$. Thus, the result of B8 has a larger jitter than B7. The reason might be that the dispersion function of B8 is larger than B7.

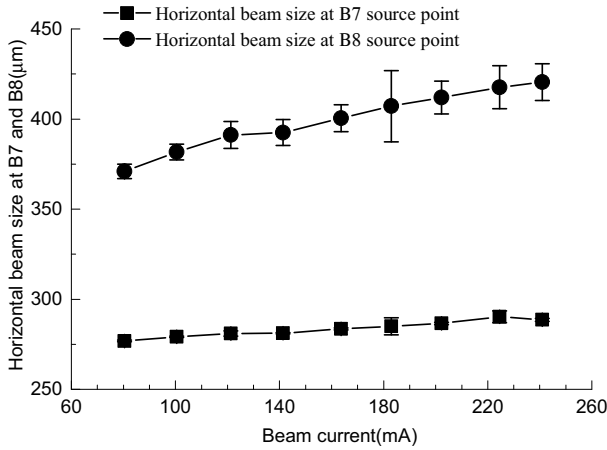


Fig. 8. The horizontal beam size(± 1 standard deviation) of the B7 source point measured by the interferometer and of the B8 source point measured by the imaging system (at multi bunch operation).

The corresponding horizontal beam emittance and the beam energy spread are inferred(Fig. 9). The horizontal beam emittance at 220 mA is obviously extraordinary($36.24 \text{ nm}\cdot\text{rad}$). The rest point give a mean value of $35.04 \pm 0.24 \text{ nm}\cdot\text{rad}$. The relative beam energy spread has a positive correlation with the beam current(from 80 mA to 240 mA).

In order to precisely measure the beam size when the beam current is more than 240 mA, a new double slit

with a less separation will be utilized. And the longitudinal beam feedback system should be optimized to make sure that the beam is stable.

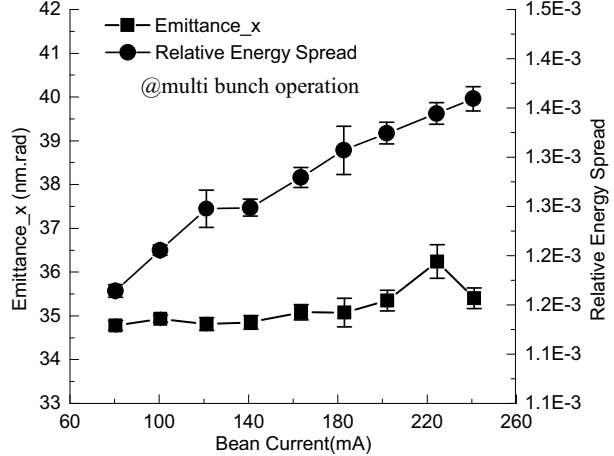


Fig. 9. Horizontal emittance and beam relative energy spread(± 1 standard deviation) measured by the interferometer system and the imaging system(at multi bunch operation).

4 Conclusion

Two transverse beam profile measurement systems using visible SR have been installed at HLS II storage ring. One is a SR interferometer system consisted of two channels. Another is a simple imaging system which can monitor the beam transverse profile directly. Oxygen-free copper mirrors is applied to prevent thermal deformations from the SR heat load.

Simulations of these two optic systems were finished using SRW. The simulation results are consistent with the theoretic value. And the σ -polarized component of SR can be used in measurement.

Measurement of beam size at different beam current at single bunch operation are obtained. The vertical beam size agrees with the theoretic value at 10% coupling coefficient and the horizontal beam size is larger than the theoretic value. With combining the interferometer system and imaging system, the horizontal beam emittance and the beam energy spread are inferred.

References

- 1 G Kube. Review of Synchrotron Radiation based Diagnostics for Transverse Profile Measurements. In *Proceedings of DIPAC 2007*, pages 6–10, Venice, Italy, 2007.
- 2 S Takano. Beam diagnostics with synchrotron radiation in light sources. In *Proceedings of IPAC 2010*, pages 2392–2396, Kyoto, Japan, 2010.
- 3 T Naito and T Mitsuhashi. Improvement of the Resolution of SR Interferometer at KEK-ATF Damping Ring. In *Proceedings of IPAC 2010*, volume 6, pages 972–974, Kyoto, Japan, 2010.
- 4 L L Tang. *Development and Study of Beam Profile Measurement System for HLS II*. PhD thesis, University of Science and Technology of China, 2013.
- 5 T Mitsuhashi. Spatial coherency of the synchrotron radiation at the visible light region and its application for the electron beam profile measurement. In *Proceeding of PAC of 1997*, volume 1, pages 766–768. IEEE, 1997.
- 6 T Mitsuhashi and T Naito. Measurement of beam size at the ATF damping ring with the SR interferometer. In *Proceeding of sixth EPAC*, volume 22, pages 1565–1567, Stockholm, Sweden, 1998.

- 7 T Mitsuhashi. Measurement of Small Transverse Beam Size Using Interferometry. In *Proceedings DIPAC 2001*, ESRF, Grenoble, France, 2001.
- 8 T Mitsuhashi. Twelve Years of SR Monitor Development at KEK. In *Proceedings of BIW 2004*, Oak Ridge, Tennessee, 2004.
- 9 P Chevtsov, A Day, J Denard, et al. Non-invasive energy spread monitoring for the JLAB experimental program via synchrotron light interferometers. *Nuclear Instruments and Methods in Physics Research Section A*, 557(1):324–327, 2006.
- 10 J Corbett, W Cheng, A Fisher, et al. Interferometer Beam Size Measurements in SPEAR3. In *Proceedings PAC 2009*, Vancouver, BC, Canada, 2009.
- 11 S T Wang, D L Rubin, J Conway, et al. Visible-light beam size monitors using synchrotron radiation at CESR. *Nuclear Instruments and Methods in Physics Research Section A: Accelerators, Spectrometers, Detectors and Associated Equipment*, 703:80–90, 2013.
- 12 J Chen, K R Ye, and Y B Leng. Development of Shanghai Synchrotron Radiation Facility synchrotron radiation interferometer. *HIGH POWER LASER AND PARTICLE BEAMS*, 23(1):179–184, 2011.
- 13 L L Tang, B G Sun, Y Y Xiao, et al. The measurement of electron beam transverse sizes by synchrotron radiation interferometry for HLS II. *Nuclear Science and Techniques*, 8.23(4):193–198, 2012.
- 14 Å Andersson, M Böge, A Lüdeke, V Schlott, and A Streun. Determination of a small vertical electron beam profile and emittance at the Swiss Light Source. *Nuclear Instruments and Methods in Physics Research Section A: Accelerators, Spectrometers, Detectors and Associated Equipment*, 591(3):437–446, 2008.
- 15 A Hansson, E Wallén, and Å Andersson. Transverse electron beam imaging system using visible synchrotron radiation at MAX III. *Nuclear Instruments and Methods in Physics Research Section A*, 671:94–102, 2012.
- 16 J Corbett, W Cheng, A Fisher, et al. Interferometer Beam Size Measurements in SPEAR3. In *Proceedings PAC 2009*, Vancouver, BC, Canada, 2009.
- 17 L Wang, J X Zhao, J S Cao, et al. Beam size measurement of BEPC II storage ring by using visible synchrotron light interferometry. *HIGH POWER LASER AND PARTICLE BEAMS*, 23(9):2512–2514, 2011.
- 18 M Masaki and S Takano. Two-dimensional visible synchrotron light interferometry for transverse beam-profile measurement at the SPring-8 storage ring. *Journal of synchrotron radiation*, 10(4):295302, 2003.
- 19 T Naito and T Mitsuhashi. Very small beam-size measurement by a reflective synchrotron radiation interferometer. *Physical Review Special Topics-Accelerators and Beams*, 9(12):122802, 2006.
- 20 K Tang, J G Wang, B G Sun, et al. Beam transverse size and emittance measurement of HLS II using interferometry. *HIGH POWER LASER AND PARTICLE BEAMS*, 27:245–249, 2014.
- 21 O Chubar, P Elleaume, S Kuznetsov, et al. Physical optics computer code optimized for synchrotron radiation. In *International Symposium on Optical Science and Technology*, pages 145–151. International Society for Optics and Photonics, 2002.